Wavelet analysis of auditory evoked potentials recording human vertex responses (Image analysis and multidmensional wavelet analysis)

AUTHOR(S):

Ikawa, Nobuko; Morimoto, Akira; Ashino, Ryuichi

Wavelet analysis of auditory evoked potentials recording human vertex responses

Nobuko Ikawa
Ryutsu Keizai University*
Akira Morimoto and Ryuichi Ashino
Osaka Kyoiku University†

Abstract

This paper describes the wavelet analysis of auditory evoked potentials, such as auditory brainstem responses (ABRs) and auditory steady-state responses (ASSRs). Because ABRs are examined using the peak amplitudes and latencies of waveforms in hearing diagnosis, one-dimensional discrete stationary wavelet analysis (DSWA) is beneficial for analyzing ABRs. Power spectrum analysis and phase coherence analysis using one-dimensional complex continuous wavelet analysis (CCWA) are useful for the detection of ASSRs because of their sinusoidal waveform configuration.

1 Introduction

It is well known that Helen Adams Keller tried her utmost to acquire language skills. For infants who are hard of hearing, the earlier they are diagnosed by a hearing test, the more language skills they acquire in later life. Nowadays, all newborn infants have an automated auditory brainstem response (ABR) hearing test (see [9]). If an infant does not pass the test, he or she then has the auditory steady-state response (ASSR) hearing test. In these tests, electroencephalogram (EEG) signals such as ABR and ASSR waveforms are commonly used.

*120 Ryugasaki-shi, Ibaraki, 301-8555, Japan
E-mail address:ikawa@rku.ac.jp
†Kashiwara-shi, Osaka, 582-8582, Japan

Unfortunately, the automated ABR hearing test takes about 15 min and the ASSR hearing test takes about 30 min. Furthermore, all newborn infants have the automated ABR hearing test during sleep. When an infant has the ASSR hearing test, the infant must often be under anesthesia (sedative). For these reasons, reducing the test times of the automated ABR and ASSR hearing tests is desirable.

Tasks:

- Propose a method of signal processing for accurate detection of ABR and ASSR waveforms.
- Shorten the analysis time of ABR and ASSR waveforms to reduce the time of audiometry tests.

Solutions:

- Use optimal wavelet analysis for accurate detection of ABRs and ASSRs.
- For ABRs and ASSRs, through the observation on the way of averaged waveforms, propose a waveform processing model of gradual detection.

2 ABR and ASSR waveform

2.1 ABR waveform

An ABR is evoked as the human brain response by input sound stimulation from the ears during the 10 ms. An ABR has seven peaks, and the formation of waves I, II, III, IV and V originates in specific parts of the auditory neural system in the brainstem (shown in Figures 1 and 2). The time (latency) and amplitude analyses of these waveforms supply information on the peripheral hearing status and the integrity of the brainstem pathway.

Therefore, the ABR is one of the important indicators for human objective audiometry. The ABR has been obtained by averaging many waveforms, sometimes as many as about $2,000$. The waveform shown in Figure 1 has already been averaged.

Definition

During the 10 ms of input sound stimulation from the ears, we obtain a data sequence called Epoch, with the kth epoch denoted by Epoch_k. We define

$$\text{ABR}_N = \frac{1}{N}\sum_{k=1}^{N} \text{Epoch}_k.$$

We call ABR_N the N-average ABR, which we hereafter refer to as the ABR.

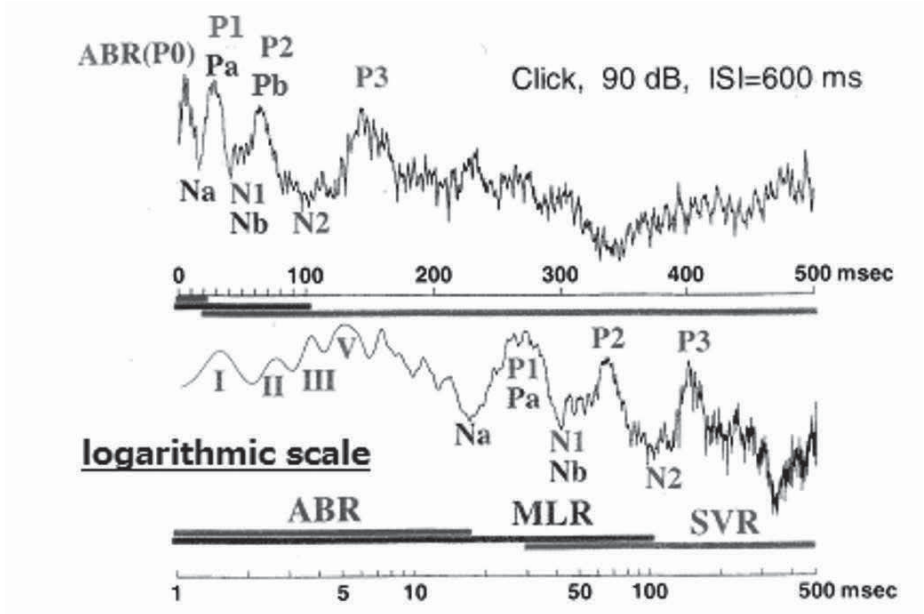

Figure 1: Waveforms and latencies of ABR and ASSR of auditory pathway [1].

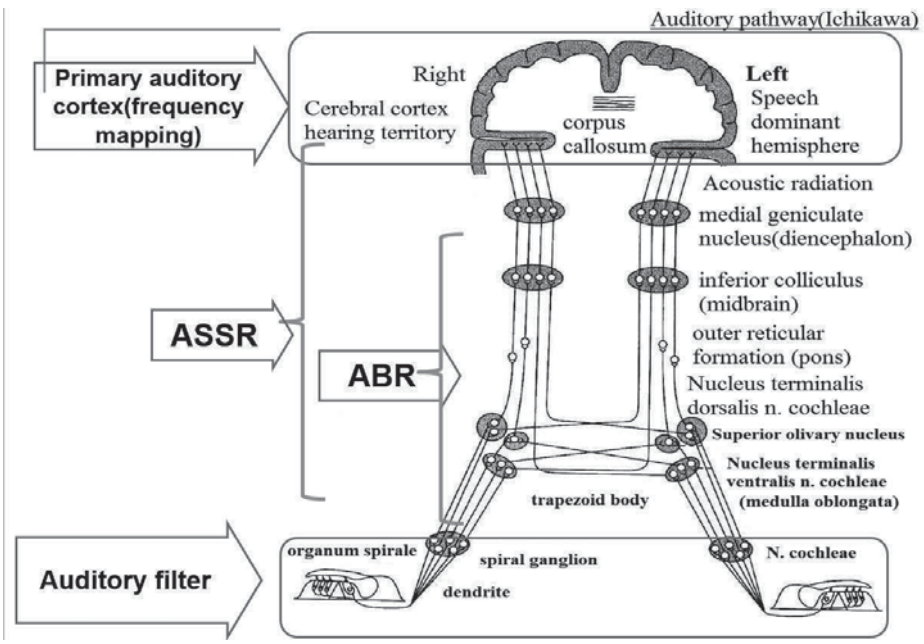

Figure 2: ABR and ASSR of auditory pathway [10].

The ABRs used in this paper were recorded in an acoustically quiet room. Subjects reclined in a comfortable chair or lay on a bed. An electrode was placed high on each subject's vertex. Two electrodes were placed on the earlobes of both ears. A ground electrode was placed on the forehead. The subjects were healthy 20-year-old males.

As input stimuli, we used acoustic stimuli composed of clicks with an intensity of 70 dB nHL, a duration of 0.1 ms and a frequency of 20 Hz. Here, the decibel normal-hearing level (dB nHL) values are with reference to the hearing thresholds of normal hearing subjects. We stored 512-point EEG data after the click stimulus. Each set of 512 points of data is called an epoch. The duration of one epoch is 10.24 ms since the sampling rate is $50,000$ Hz.

We should take the effects of subject gender, age and input stimulus conditions into account when we detect the peak latencies of ABR_N from the observed ABR_N waveforms. That is, younger or female subjects generally show larger wave amplitudes and earlier wave latencies, and older or male subjects generally show smaller wave amplitudes and later wave latencies, particularly for waves corresponding to ABR_N waves III and V.

The following is a general method of extracting for peak latencies. We determine the template ABR_N waveform on the basis of the detection rule of the ABR_N peak characteristics for the latency shift. This rule depends on the conditions of gender, age and stimulus. Then, we extract the peak latencies of ABR_N waveforms according to the template.

We previously established a rule database for template ABR_N waveform selection using these factors as input parameters ([11]). That is, we decided the rule for choosing the most suitable template ABR_N waveform under these conditions. In our examination, we obtained data from the healthy 20-year-old males.

Figure 3 shows four examples of normal ABR_N waveform types classified with respect to waves IV and V, obtained using $2,000$ averagings and clicks with an intensity of 80 dB nHL, a duration of 0.1 ms and a frequency of 20 Hz as the stimulus.

Figure 4 shows an example of the normal ABR_N waveforms obtained with various intensities of 80, 70, 60, 50 and 40 dB nHL in the case of type 1. Each pair of overlapping graphs show the responses of the left and right ears.

2.2 ASSR waveform

Next, we discuss ASSRs according to the well known assertion, that an ASSR is composed of a slow ABR and a middle-latency response (MLR) (see Figure 5, [1] and [6]). To assess the clinical hearing level of infants, the MAS-

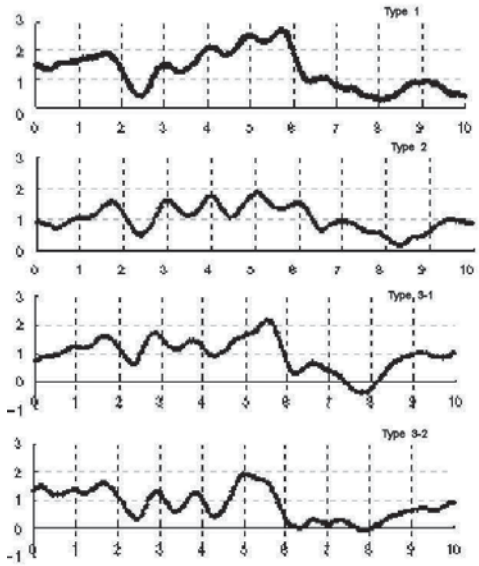

Figure 3: Normal ABR_N waveform types classified with respect to waves IV and V, obtained with $N = 2000$ averagings.

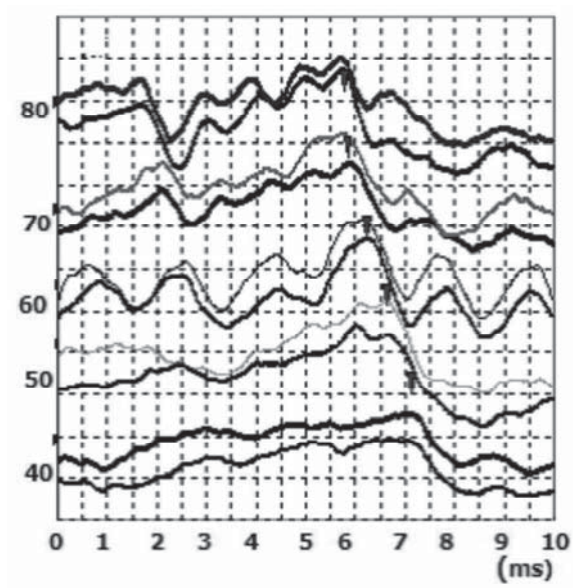

Figure 4: Example of normal ABR_N waveforms (overlapping left and right ear responses) obtained from input stimuli with intensities of 40, 50, 60, 70 and 80 dB nHL.

TER (multiple auditory steady-state evoked response [24]) and Navigator PRO systems are useful. These systems use the 80-Hz ASSR. It takes 30 min to test the hearing level at five frequencies,which is a long time, especially for infants or very young children. Before measuring the 80-Hz ASSR, we use a sedative because subjects must be asleep. On the other hand, the 40-Hz ASSR can be measured when subjects are awake. Therefore, a rapid objective audiometry test has been desired for the 40-Hz ASSR.

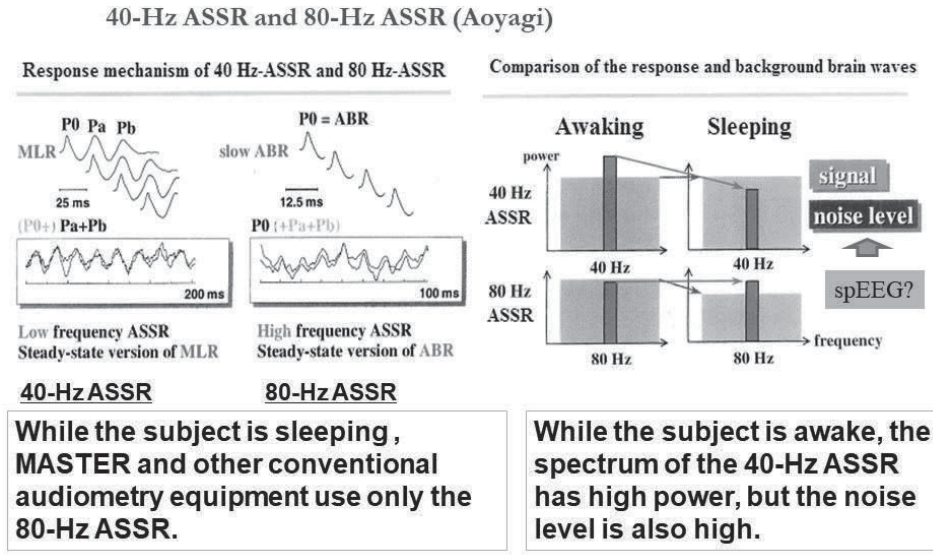

Figure 5: About ASSR configuration.

The 40-Hz ASSR was recorded using our previously proposed hardware system reported in [13]. The input stimuli (sound conditions) were sinusoidal amplitude-modulated (SAM) tones. We fixed the modulation frequency (MF) at 40 Hz and selected a single carrier frequency (CF) of $1,000$ Hz. We started with a sound intensity of 70 dB nHL. Then, we decreased the sound intensity to its threshold in steps of 10 dB nHL. For normal-hearing subjects, the 40-Hz ASSR is recorded as a waveform with the same frequency as the modulation frequency (40 Hz).

We recorded the EEG for up to 30 s. The sampling frequency was $1,024$ Hz. We cut the digital data into epochs, where one epoch consisted of 512 points of data. The duration of one epoch was 500 ms. It was necessary to average at least 20 epochs with sound stimuli above 60 dB nHL and to average at least 40 epochs with sound stimuli below 60 dB nHL. For 60 dB nHL, if we were unable to detect the 40-Hz ASSR from the average of 20 epochs, then we checked the average of 40 epochs. Since one epoch took 500

ms, we measured the EEG for 10 or 20 s.

To decrease the time required to measure the EEG using our original objective audiometry device, in this study, we design a new procedure for averaging the waveforms of the 40-Hz ASSR. Our averaging method is based on the Galambos idea shown in Figure 6. Since the sampling frequency is $1,024$ Hz, $1,024/40 = 25.6 \approx 26$ points are shifted for one period of 40 Hz.

For the sampling data $\mathrm{D} = \{d[t] \mid t = 0, 1, 2, \ldots\}$ and $m \geq 1$, we set

$$\vec{a}_k = (d[26(k-1)], d[26(k-1)+1], \ldots, d[26(k-1)+511]), \quad k = 1, \ldots, m.$$

Then, for $\mathrm{M} \leq (m - 20)$, we define the average vector as

$$\vec{s}_{\mathrm{M}} = \frac{1}{\mathrm{M}} \sum_{k=21}^{\mathrm{M}+20} \vec{a}_k. \tag{1}$$

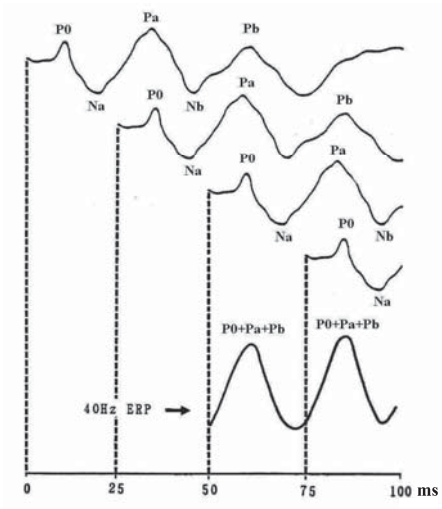

Figure 6: Relationship of the 40-Hz event-related potential (ERP) with the middle latency response [6].

3 Conventional methods

Wavelet analysis is a new time-frequency analysis or, more precisely, time-scale analysis (see [23]). Some earlier applications of wavelets to ABRs were presented by Hanrahan [7, 8]. Several applications of wavelet analysis in the

neurosciences are also given in [3]. The auditory nerve relays electrical nerve impulses from the ears to the cerebrum.

We record activities of the auditory neuron group at the midbrain as the EEG. This EEG is called an auditory evoked brain response (AEBR) or auditory evoked potentials (AEPs). AEBRs or AEPs are used in human objective audiometry tests. In the conventional methods for analyzing AEPs, Bradley and Wilson applied wavelet analysis to averaged AEP waveforms in [2, 26, 27].

Discrete stationary wavelet analysis (DSWA) is applied to the waveform analysis of AEPs. We also applied DSWA to ABRs in [11], where an ABR is one of the AEPs.

In this paper, we first focus on the analysis of ABRs. An ABR is evoked as the human brain response by input sound stimulation from the ears during the 10 ms. The ABR is one of the important indicators for human objective audiometry. The ABR has been obtained by averaging many waveforms, and the conventional methods sometimes require about $2,000$ waveforms for averaging. The method proposed by Bradley and Wilson uses $2,048$ averaged ABR data. We also observed the $2,000$ averaged ABR waveforms using DSWA.

In this section, we explain the conventional method of applying DSWA by using our obtained ABR waveform data. We obtained almost the same results as those in Wilson's papers [2, 26, 27].

3.1 Applying DSWA to ABRs

We used DSWA as the wavelet transformation (WT). We chose nine decomposition levels, that is, eight detailed scales ($D1-D8$) and a final approximation (A8), where the decomposition was performed by MATLAB software. We chose bi-orthogonal 5.5 (bior 5.5) wavelet functions (Figure 7 [25]) for DSWA. The decompositions and the frequency bands are shown in TABLE 1.

Two results of applying DSWA to ABRs were shown in Figure 8. We observed waves I, II, III, IV and V of the ABR at D5 and wave V of the ABR at D6 and D7. On the other hand, we observed wave III at A8, and this wave III had the largest amplitude in all levels.

4 Proposed method

An ABR mainly consists of two frequency components [4]: a fast ABR (high frequency component) and a slow ABR (low-frequency component). Using this fact, we propose a concurrent processing method to detect the peak

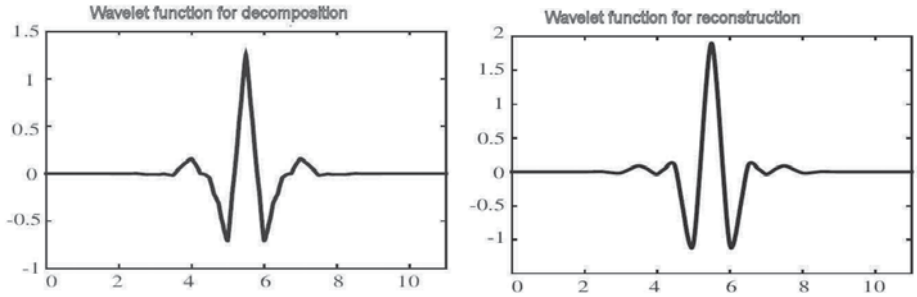

Figure 7: Decomposition and reconstruction wavelet functions of bior 5.5.

Table 1: Relationship between details and approximation and frequency ranges.

Details and approximation	Our frequency band
D1	12,500 – 25,000 Hz
D2	6,250 – 12,500 Hz
D3	3,125 – 6,250 Hz
D4	1,562 – 3,125 Hz
D5	**781 – 1,562 Hz**
D6	390 – 781 Hz
D7	195 – 390 Hz
D8	97 – 195 Hz
A8	0 – 97 Hz

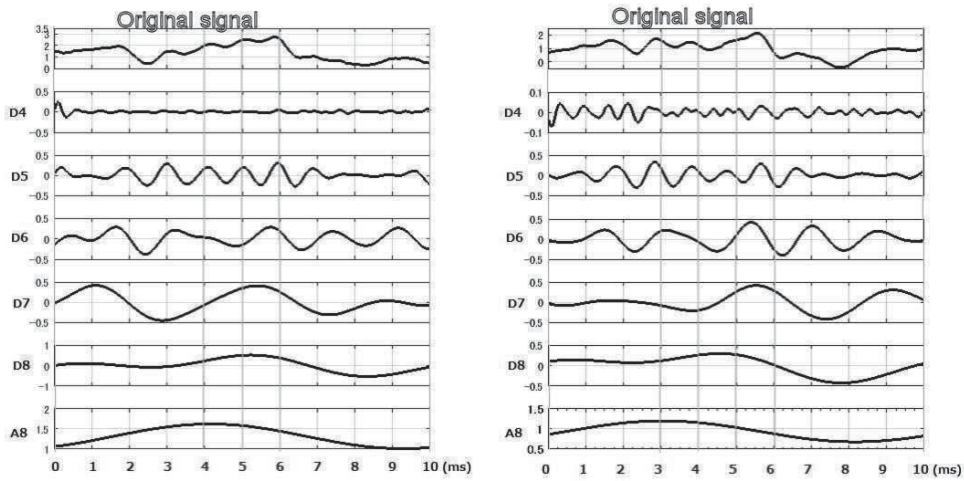

Figure 8: Examples of results of applying DSWA to ABRs.

latencies of an ABR waveform in a short time. The fast ABR can be obtained by averaging only 10 waveforms. In [11, 15, 16], we proposed a new method that uses only 10 averaged ABRs. Our proposed method detects peak latencies six times faster than the conventional methods and reduces the observation time.

On the other hand, the slow ABR seems to be a spontaneous electroencephalographic (spontaneous EEG) synchronization signal. We explain the synchronization signal by using the Kuramoto model (see [20, 21]). To obtain the slow ABR, it is necessary to average 300 waveforms. We propose a method of concurrently detecting both the fast and slow ABRs.

4.1 Apply DSWA to averaging ABR_N

In the previous section, we analyzed the ABRs obtained as a result of averaging many waveforms ("epochs"):

$$\mathrm{ABR}_N = \frac{1}{N}\sum_{k=1}^{N} \mathrm{Epoch}_k, \tag{2}$$

where an "epoch" consists of 512 points of sampling data x_0, x_1, x_2, $\cdots$, x_{511} in the AEP during 10.24 ms. Epoch_k denotes the kth epoch:

$$\mathrm{Epoch}_k = (x_{k0}, x_{k1}, x_{k2}, \cdots, x_{k511}). \tag{3}$$

We use ABR_N to denote an N-average ABR.

We apply DSWA not only to average an ABR but also in each process of averaging waveforms. Here, SWT denotes a discrete stationary wavelet transform and ISWT denotes its inverse discrete stationary wavelet transform. We have the following decomposition of ABR_N:

$$\mathrm{ABR}_N = \mathrm{ISWT}(\mathrm{SWT}(\mathrm{ABR}_N)) = \sum_{i=1}^{8} \mathrm{D}i_N + \mathrm{A8}_N, \tag{4}$$

where $\mathrm{D}i_N$ and $\mathrm{A8}_N$ denote the ith detail and the eighth approximation of ABR_N, respectively. In the previous section, we analyzed $\mathrm{ABR}_{2,000}$.

In this section, we study the dependence of ABR_N on N for $N = 10$, 20, 30, 40, 100, 200, 300, 1000, 1500, 2000 by observing $\mathrm{D}i_N$, $i = 1, 2, \cdots, 8$ and $\mathrm{A8}_N$. In Figure 9 and 10, the overlapped graphs show $\mathrm{D}i_N$, $i = 4, 5, \cdots, 8$ and $\mathrm{A8}_N$, respectively.

In Figure 9, we observed the typical peak latency of wave V ($\mathrm{PL_V}$) in $\mathrm{D5}_N$ for all $N = 10$, 20, 30, 40, 100, 200, 300, 1000, 1500, 2000. In the time interval $[5, 6.5]$ ms, there was a negligible difference among $\mathrm{D5}_N$ for all N.

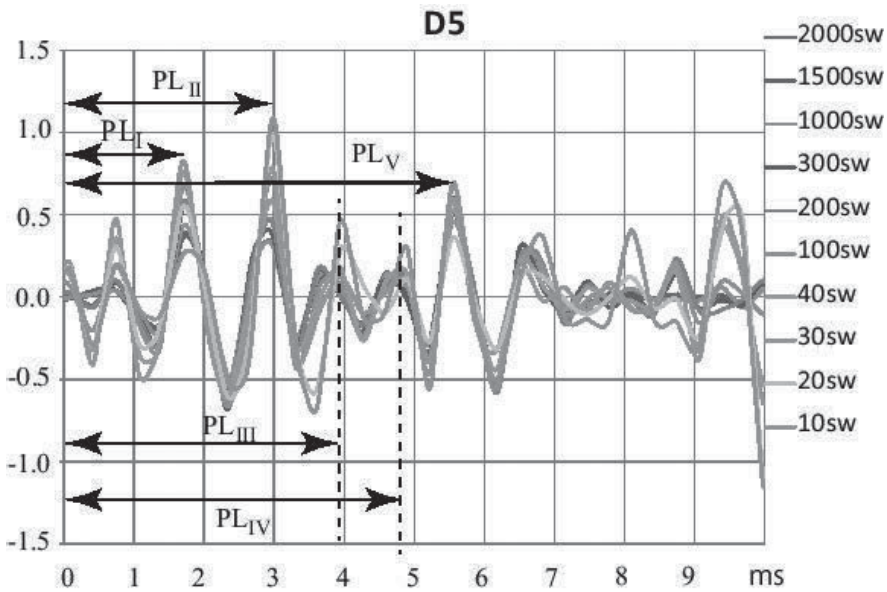

Figure 9: $\mathrm{D5}_N$, $N = 10$, 20, 30, 40, 100, 200, 300, 1000, 1500, 2000. For $\mathrm{D5}_{10}$, we can detect peak latencies $\mathrm{PL_I}$, $\mathrm{PL_{II}}$, $\mathrm{PL_{III}}$, $\mathrm{PL_V}$.

Even when $N = 10$, we can already detect the peak latency of wave V using the graph of $\mathrm{D5}_N$ (see the peak at about 5.5 ms). As N increases, the

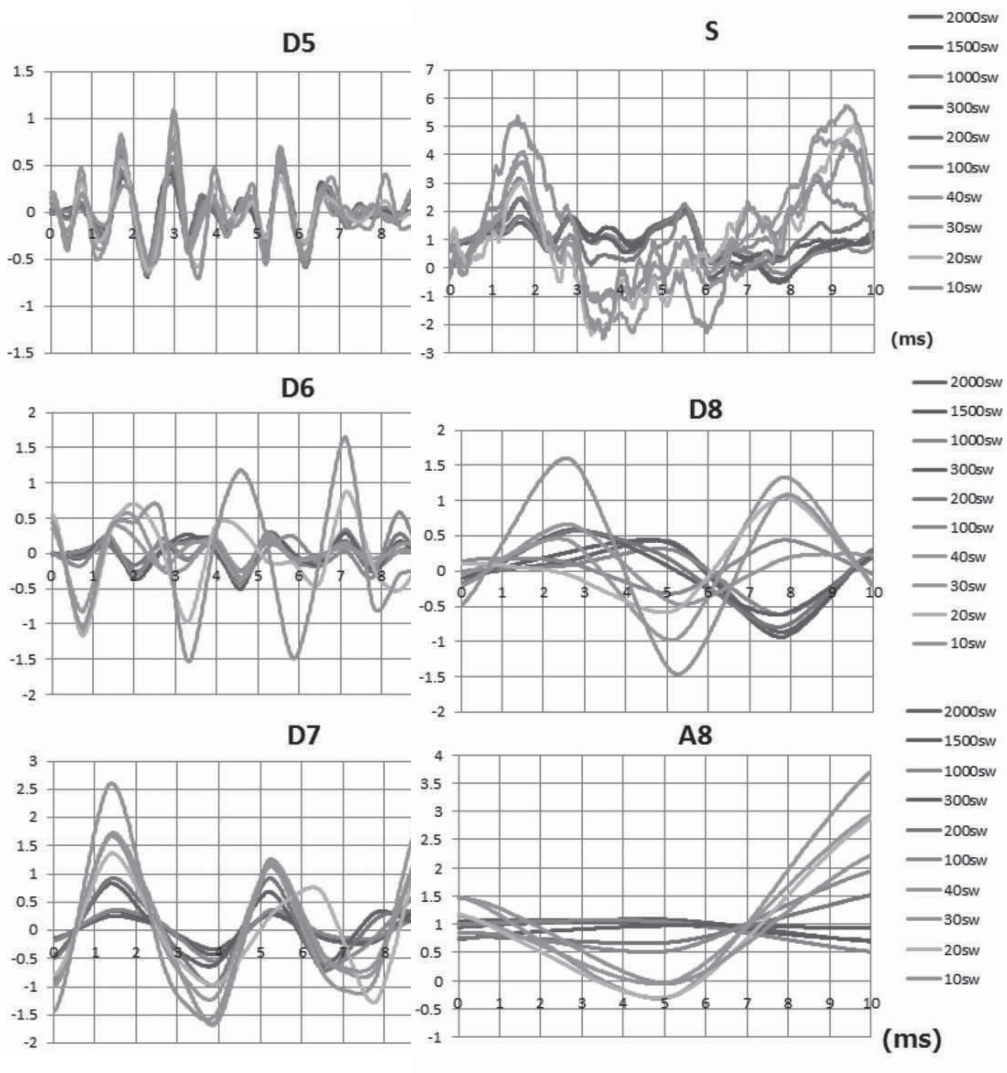

Figure 10: S_N (original signal ABR_N) and Di_N, $i = 4, 5, \cdots, 8$, $A8_N$ for each $N = 10, 20, 30, 40, 100, 200, 300, 1000, 1500, 2000$.

peak latency of wave V at 5.5 ms does not change and the phase of about 5.5 ms is locked. We consider that wave V belongs to the fast ABR. Figure 9 shows that we can detect peak latencies PL_{I}, PL_{II}, PL_{III} and PL_{V} from $D5_{10}$.

On the other hand, for $N \geq 300$, we can find the peak latency of wave III in the graph of $A8_N$ (the peak at about 4 ms at the bottom of Figure 10). We consider that wave III belongs to the slow ABR. For all N, wave III of $A8_N$ has the largest amplitude. If we need to observe the envelope of an ABR, then we recommend the observation of $A8_N$ for $N \geq 300$.

4.2 Kuramoto model

Using a model of the synchronization phenomenon, we explain the relation Di_N, $i = 1, 2, \cdots, 8$ and $A8_N$ (see [20, 21]). We consider N coupled phase oscillators according to the Kuramoto model:

$$\frac{d\theta_i}{dt} = \omega_i - \frac{K}{N}\sum_{j=1}^{N} \sin(\theta_i - \theta_j), \ i = 1, \cdots, N, \tag{5}$$

where $\theta_i(t)$ is the phase of the ith oscillator, which has the natural frequency ω_i. The non-negative constant K is the coupling strength among the oscillators.

From computer simulations, the following are known:

- For $K = 0$, each oscillator oscillates with the natural frequency (**asynchronous state**).
- For $K > K_s$, the oscillators synchronize with each other. That is, each $\theta_i(t)$ has the same time average (**synchronized state**).

Let $\theta_1(t)$, $\theta_2(t)$ and $\theta_3(t)$ be the phases of D5, D6 and A8, respectively, and ω_i denote the natural frequency of $\theta_i(t)$, $i = 1, 2, 3$.

The results of computer simulations are illustrated in Figure 11, where we plot the differences $\theta_i(t) - \omega_i t$ for $K = 0, 0.06, 0.12, 0.18$.

Using the sine wave fitting algorithm in [5], we conclude that the natural frequencies of A8, D6 and D5 are $\omega_3 = \pi/250$, $\omega_2 = \pi/50$ and $\omega_1 = \pi/25$, respectively. The larger the value of K, the slower $\theta_1(t)$ and $\theta_2(t)$ change. However, the larger the value of K, the faster $\theta_3(t)$ changes.

From the results in Figure 11, we can presume the model shown in Figure 12. We assume that the stimulation-induced neuron group produces the fast ABR (D5, D6) and that the spontaneous EEG neuronal group produces the slow ABR (A8). That is, a fast ABR can show the transmitted signal of the input stimulus. On the other hand, it is presumed that the slow ABR is formed while synchronizing with a spontaneous EEG neuronal group.

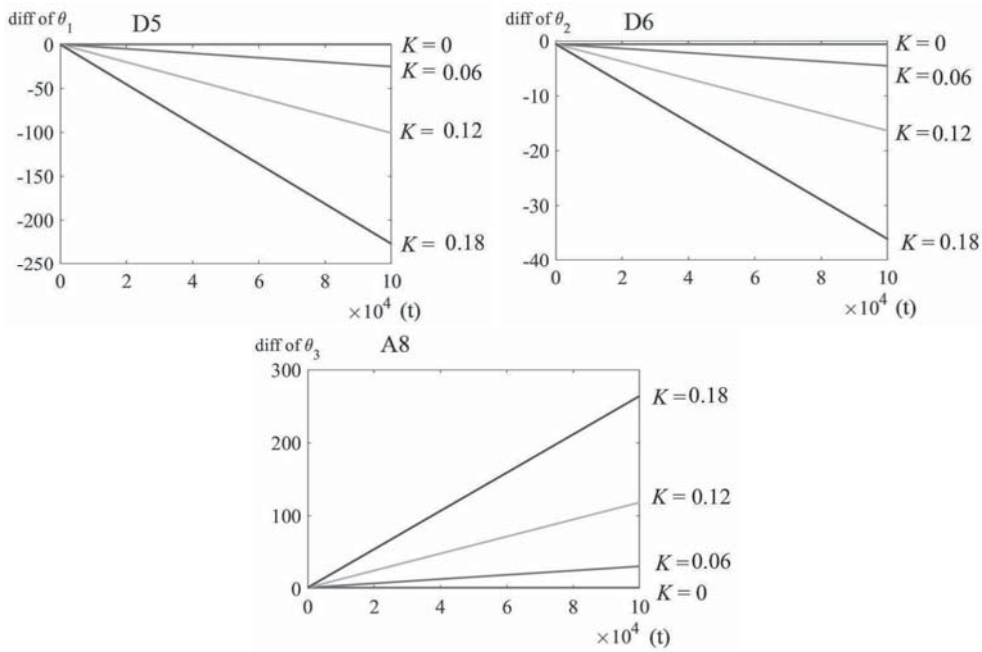

Figure 11: Simulation results of the Kuramoto model. Upper: $\theta_1(t) - \omega_1 t$ as D5, middle: $\theta_2(t) - \omega_2 t$ as D6 and lower: $\theta_3(t) - \omega_3 t$ as A8.

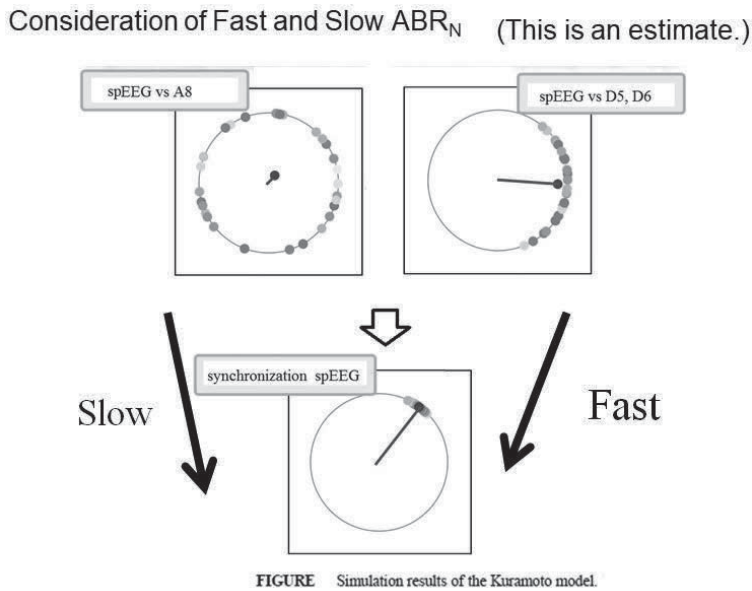

Figure 12: Estimation of behavior of slow and fast ABR_N.

4.3 New detection method

In the conventional detection methods, peak latencies are detected by using $\mathrm{ABR}_{2,000}$, where it is necessary to average $2,000$ epochs. Thus, it takes a long time to detect peak latencies.

On the other hand, as shown in subsection 4.1, we can detect the peak latency of wave V using $\mathrm{D5}_{10}$. We can also detect the peak latency of wave III using $\mathrm{A8}_{300}$. For the fast ABR, it is necessary to average a very small number of epochs, whereas for the slow ABR, it is necessary to average many epochs.

We propose the concurrent processing method shown in Figure 13. This method changes the number of epochs to be averaged according to whether the fast or slow ABR is being considered. Our proposed method can detect peak latencies faster than the conventional methods.

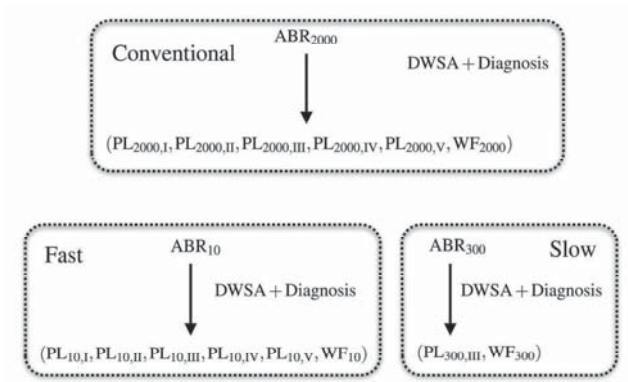

Figure 13: Comparison between the conventional detection methods and the proposed method.

5 One-dimensional complex continuous wavelet analysis

Next, we apply complex continuous wavelet analysis (CCWA) to ABRs and ASSRs. Several experiments have shown that an ABR consists of three groups in the time domain. We propose the use of a new hearing test based on CCWA as a possible faster alternative.

By observing the results of applying CCWA to ASSRs, we propose a new averaging method based on the Galambos idea (see [6] and [22]). We carry out several experiments to demonstrate that our proposed method is seven

times faster than the conventional methods.

A mother wavelet is a function $\psi \in L^2(\mathbb{R})$ with zero average: $\int_{-\infty}^{+\infty} \psi(t)\, dt = 0$. TYpically, it is normalized, $\|\psi\| = 1$, and centered in the neighborhood of $t = 0$. For $a > 0$ and $b \in \mathbb{R}$, we define

$$\psi_{a,b}(t) = \frac{1}{\sqrt{a}}\, \psi\left(\frac{t-b}{a}\right). \tag{6}$$

Note that $\|\psi_{a,b}\| = 1$. The continuous wavelet transform of $x \in L^2(\mathbb{R})$ at (a, b) is defined by

$$W_\psi[x(t)](a,b) = C(a,b) = \langle x, \psi_{a,b}\rangle = \int_{-\infty}^{\infty} x(t)\psi^*_{a,b}(t)\, dt, \tag{7}$$

where ψ^* denotes the complex conjugate of ψ. For the mother wavelet, we choose the complex Morlet wavelet function $\psi(t)$ defined by

$$\psi(t) = \frac{1}{\sqrt{2\pi\sigma^2}} e^{-\frac{t^2}{2\sigma^2}} e^{i\omega_0 t}, \tag{8}$$

which is illustrated in Figure 14. The real part $\Re\psi(t)$ of $\psi(t)$ is reflection-symmetric about $t = 0$. The imaginary part $\Im\psi(t)$ of $\psi(t)$ is point-symmetric about $(0, 0)$. Here, we set $\sigma = \frac{\sqrt{3}}{2}$, $\omega_0 = 2\pi$ and use the MATLAB function

```
[PSI,X] = cmorwavf(LB,UB,N,FB,FC)
```

for the complex Morlet wavelet with `LB=-5`, `UB=5`, `N=1000`, `FB=1.5`, and `FC=1`. In this paper, the wavelet analysis using the Morlet wavelet is called one-dimensional CCWA.

5.1 Application of CCWA to ABRs

Figure 15 shows the results of applying CCWA to two normal ABRs. Each waveform (upper graph) is the original waveform of the ABR. Each intensity image (lower graph) shows the modulus of the continuous wavelet transform $C_{a,b} = C(a, b)$. White painting indicates a high modulus and black painting indicates a low modulus. The horizontal axis indicates time from 0 to 10 ms. These graphs show the typical characteristics of the peaks of two normal ABR waveforms.

From the results of CCWA, we observed that each ABR waveform has three frequency groups. The first group consists of the time interval from 0 to 3 ms, the second group consists of the time interval from 3 to 7 ms and the third group consists of the time interval from 7 to 10 ms. Furthermore,

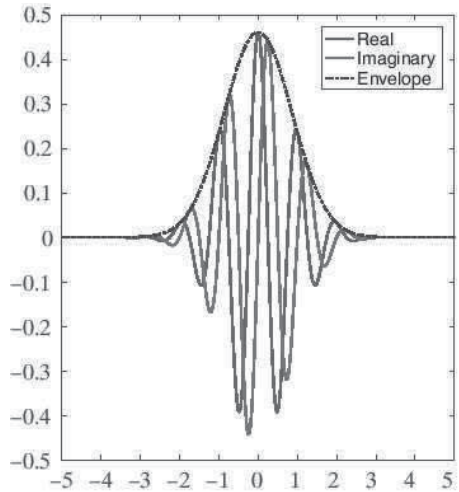

Figure 14: Complex Morlet wavelet.

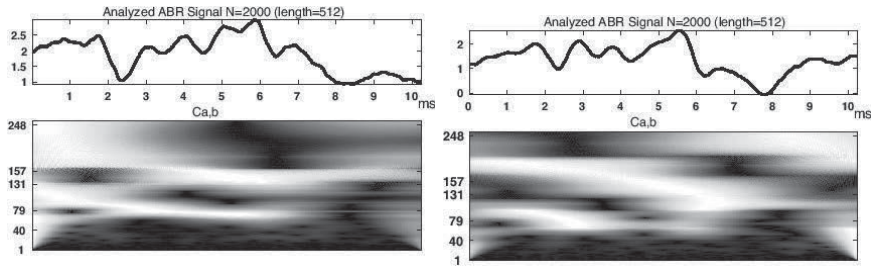

Figure 15: Application of CCWA to ABRs. The upper ABR has the fourth peak at 5 ms, whereas the lower ABR does not have this peak.

the second band has two white painted frequency bands. However, there is a difference between the two images showing the modulus. The different frequencies around 5 ms indicate whether the fourth peak in the ABR exists.

5.2 Application of CCWA to ASSRs

We carried out the following two observations. In the first step, we applied CCWA to spontaneous EEG (non-evoked) waveforms. The CCWA results are shown in Figure 16, where the result of one epoch waveform $\vec{a}_1$ is shown in the left graph, and the averaged spontaneous EEG $\vec{S}_{40}$ is shown in the right graph. We can observe brain waves of periodic frequency but we cannot observe 40-Hz waves. In Figure 16, white painting indicates a high modulus and black painting indicates a low modulus.

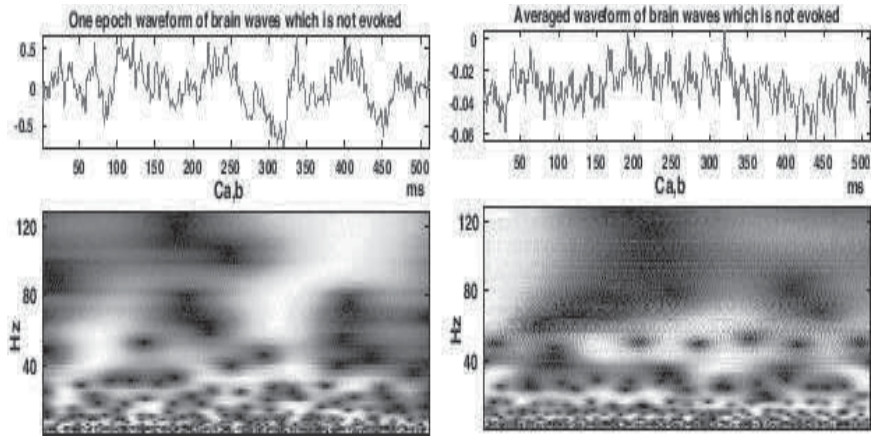

Figure 16: Application of CCWA to non-evoked brain waveforms (spontaneous EEG waveforms). Left: one epoch $\vec{a}_1$. Right: averaged vector $\vec{S}_{40}$.

In the second step, we applied CCWA to auditory evoked brain waveforms. The results are shown in Figure 17, where the CCWA results of one epoch waveform $\vec{a}_1$ with 70, 50, 30 dB nHL are illustrated on the left side. We cannot observe 40-Hz waves. The CCWA results of the average vector are illustrated on the right side of Figure 17, in which we can observe 40-Hz waves. We use $\vec{S}_{20}$ for 70 dB nHL and $\vec{S}_{40}$ for 50 and 30 dB nHL.

In our experiments we demonstrate that we can detect 40-Hz ASSR by using $\vec{S}_{20}$ when sound stimuli above 60 dB nHL and that we can detect a 40-Hz ASSR by using $\vec{S}_{40}$ below 60 dB nHL. Therefore, we can detect a 40-Hz ASSR enough by recording the EEGs for 1.5 or 2 s. Thus, our new averaging method is seven times faster than the conventional methods.

6 Conclusions

We applied DSWA to ABRs and ascertained that an ABR consists of fast and slow ABRs. Our simulation suggested that the stimulation-induced neuron group produces the fast ABR, and that the spontaneous EEG neuronal group produces the slow ABR. We proposed a concurrent processing method to detect peak latencies of an ABR. This method detects peak latencies faster than the conventional methods.

From the graphs obtained by applying CCWA to ABRs and ASSRs, we obtained the time-frequency characteristics of waveforms. An ABR consists of three groups in the time domain, where each group consists of multiple frequency bands.

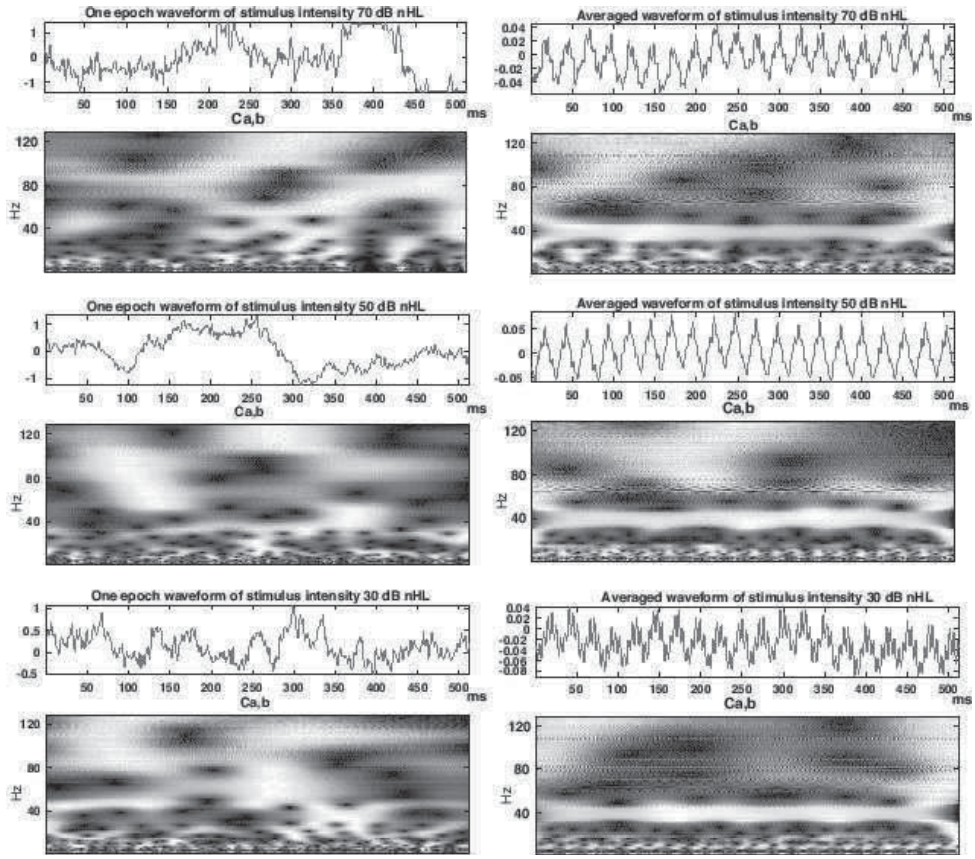

Figure 17: Application CCWA to 40-Hz ASSRs. Left: one epoch $\vec{a}_1$. Right: average vectors $\vec{S}_{20}$ for 70 dB nHL and $\vec{S}_{40}$ for 50 and 30 dB nHL.

In the case of 40-Hz ASSRs, for one epoch waveform, we did not observe the typical response around 40 Hz when all subjects received the sound stimuli. This means that the procedure of averaging epochs is essential for the detection of a 40-Hz ASSR. We proposed an averaging method based on the Galambos idea that a 40-Hz ASSR can be detected using $\vec{S}_{20}$ with sound stimuli above 60 dB nHL and a 40-Hz ASSR can be detected using $\vec{S}_{40}$ below 60 dB nHL. Our proposed method is seven times faster than the conventional methods. The automated detection of ABRs and ASSRs using CCWA is a future work.

Acknowledgements

We sincerely thank the anonymous reviewers for their helpful comments. The investigation reported in this paper was supported by CFME of Chiba University. This work was partially supported by JSPS KAKENHI Grant Numbers JP17K05298 and JP17K05363 and by the Research Institute for Mathematical Sciences, an International Joint Usage/Research Center located in Kyoto University.

References

[1] M. Aoyagi, *Auditory steady state responses (ASSR)*, Audiology Japan, **49** No.2, 135–145, (2006).

[2] A. P. Bradley, and W. J. Wilson, *On wavelet analysis of auditory evoked potentials*, Clinical Neurophysiology, **115**, 1114–1128, (2004).

[3] T. R. H. Cutmore, *The use of wavelets for auditory brain-stem analysis: advocacy and precautions*, Clinical Neurophysiology, **115(5)**, 998–1000, (2004).

[4] H. Davis, *Principles of electric response audiometry*, Ann. Otol. Rhinol. Lar., **85(Suppl. 28)**, 1–96, (1976).

[5] K. Dewi, N. Ikawa, T. Yahagi, Y. Suzuki and M. Aoyagi, *Averaging of auditory steady-state response waveforms using Kalman filter*, Proceedings of the 2007 RISP International Workshop on Nonlinear Circuits and Signal Processing (NCSP07), China, 465–468, (2007).

[6] R. Galambos, *et al.*, *A* 40*-Hz auditory potential recorded from the human scalp*, Proc. Natl. Acad. Sci. U.S.A. **78(4)**, 2643–2647, (1981).

[7] H. E. Hanrahan, *Extraction of features in auditory brain-stem response (ABR) signals*, In: COMSIG 90, Proceedings of the Third South African Conference on Communication and Signal Processing, IEEE 90TH0314-5/90, 61–66, (1990).

[8] H. E. Hanrahan, *A family of wavelets which are dilatable by simple IIR filters*, In: International Conference on Acoustics, Speech and Signal Processing, IEEE 0-7803-0532-9/92, 285–288, (1992).

[9] B. S. Herrmann, *et al.*, *Automated infant hearing screening using the ABR: Development and Validation*, American Journal of Audiology **4(2)**, 6–14, (1995).

[10] G. Ichikawa ed., *Atlas of auditory evoked response for beginners*, Hirokawa Book Store, in Japanese, (1989).

[11] N. Ikawa, T. Yahagi and H. Jiang, *Waveform analysis based on latency-frequency characteristics of auditory brainstem response using wavelet transform*, Journal of Signal Processing **9(06)**, 505–518, (2005).

[12] N. Ikawa, *et al.*, *About short time detection method of auditory steady state response evoked by sinusoidal amplitude modulation using* 40*-Hz tone sound*, Proceedings of Autumn Meeting of the Acoustical Society of Japan, 545–548, (2009).

[13] N. Ikawa, *et al.*, *A new automated audiometry device for measurement and analysis of* 40*-Hz auditory steady-state response*, Proceedings of the NCSP'10 Conference, Waikiki, USA, 250–253, (2010).

[14] N. Ikawa, *An application of wavelet analysis to objective audiometry test using evoked brain response*, Theory and scientific applications in time-frequency analysis, RIMS Kôkyûroku 1803, 71–97, (2012).

[15] N. Ikawa, *Automated averaging of auditory evoked response waveforms using wavelet analysis*, International Journal of Wavelets, Multiresolution and Information Processing, **11(04)**, 1360009-, 1–21, (2013).

[16] N. Ikawa, A. Morimoto and R. Ashino, *The detection of the relation of the stimulus intensity-latency of auditory brainstem response using optimal wavelet analysis*, Proceedings of the 2014 International Conference on Wavelet Analysis and Pattern Recognition (ICWAPR2014) Conference, Lanzhou, China, 127–133, (2014).

[17] N. Ikawa, A. Morimoto and R. Ashino, *A phase synchronization model between auditory brainstem response and electroencephalogram using the reconstructed waveform of multi-resolution discrete stationary wavelet analysis*, Proceedings of the ICWAPR2015 Conference, Guangzhou, China, 111–116, (2015).

[18] N. Ikawa, *Characteristics and modeling of averaging waveforms of auditory brainstem response using the reconstructed waveform of the wavelet transform*, Wavelet analysis and sampling theory, RIMS Kôkyûroku 1972, 23-41, (2015).

[19] N. Ikawa, A. Morimoto and R. Ashino, *Optimum wavelet filter estimating peak latencies of auditory brainstem response waveform*, Proceedings of the ICWAPR2016 Conference, Jeju, South Korea, 189–194, (2016).

[20] N. Ikawa, A. Morimoto and R. Ashino, *Fast estimation of the peak latency of auditory brainstem response using discrete stationary wavelet analysis*, Transactions of the Japan Society for Industrial and Applied Mathematics, in Japanese, **27(2)**, 216–238, (2017).

[21] N. Ikawa, A. Morimoto and R. Ashino, *New detection method for short latency of auditory evoked potentials using stationary wavelets*, Proceedings of the ICWAPR2018, Chengdu, China, 82–88, (2018).

[22] N. Ikawa, A. Morimoto and R. Ashino, *Application of complex continuous wavelet analysis to auditory evoked brain responses*, Proceedings of the 11th ISAAC Congress, Växjö, Sweden, 543–550, (2018).

[23] S. Mallat, *A Wavelet Tour of Signal Processing, The Sparse Way*, third edition, Academic Press, MA, (2008).

[24] M. S. John, *et al.*, *MASTER: a Windows program for recording multiple auditory steady-state responses*, Comput. Methods Programs Biomed. **61**, 125–150, (2000).

[25] Mathworks, *Wavelet Toolbox*, The MathWorks, Inc., (2009).

[26] W. J. Wilson, M. Winter, G. Kerr and F. Aghdasi, *Signal processing of the auditory brainstem response investigation into the use of discrete wavelet analysis*, Proc. IEEE COMSIG, 17–22, (1998).

[27] W. J. Wilson, *The relationship between the auditory brain-stem response and its reconstructed waveforms following discrete wavelet transformation*, Clinical Neurophysiology, **115**, pp. 1129–1139, (2004).